Interferon lambda promotes immune dysregulation and tissue inflammation in TLR7-induced lupus

Rishi R. Goel[a,1], Xinghao Wang[a], Liam J. O'Neil[a], Shuichiro Nakabo[a], Kowser Hasneen[b], Sarthak Gupta[a], Gustaf Wigerblad[a], Luz P. Blanco[a], Jeffrey B. Kopp[c], Maria I. Morasso[b], Sergei V. Kotenko[d,e,f], Zu-Xi Yu[g], Carmelo Carmona-Rivera[a], and Mariana J. Kaplan[a,2]

[a]Systemic Autoimmunity Branch, National Institute of Arthritis and Musculoskeletal and Skin Diseases (NIAMS), National Institutes of Health (NIH), Bethesda, MD 20892; [b]Laboratory of Skin Biology, NIAMS, NIH, Bethesda, MD 20892; [c]Kidney Diseases Branch, National Institute of Diabetes and Digestive and Kidney Diseases, NIH, Bethesda, MD 20892; [d]Department of Microbiology, Biochemistry, and Molecular Genetics, Rutgers New Jersey Medical School, Newark, NJ 07103; [e]Center for Cell Signaling, Rutgers New Jersey Medical School, Newark, NJ 07103; [f]Center for Immunity and Inflammation, Rutgers New Jersey Medical School, Newark, NJ 07103; and [g]Pathology Core Facility, National Heart, Lung, and Blood Institute, NIH, Bethesda, MD 20892

Edited by Shizuo Akira, Osaka University, Osaka, Japan, and approved January 29, 2020 (received for review September 27, 2019)

Type III IFN lambdas (IFN-λ) have recently been described as important mediators of immune responses at barrier surfaces. However, their role in autoimmune diseases such as systemic lupus erythematosus (SLE), a condition characterized by aberrant type I IFN signaling, has not been determined. Here, we identify a nonredundant role for IFN-λ in immune dysregulation and tissue inflammation in a model of TLR7-induced lupus. IFN-λ protein is increased in murine lupus and IFN-λ receptor (Ifnlr1) deficiency significantly reduces immune cell activation and associated organ damage in the skin and kidneys without effects on autoantibody production. Single-cell RNA sequencing in mouse spleen and human peripheral blood revealed that only mouse neutrophils and human B cells are directly responsive to this cytokine. Rather, IFN-λ activates keratinocytes and mesangial cells to produce chemokines that induce immune cell recruitment and promote tissue inflammation. These data provide insights into the immunobiology of SLE and identify type III IFNs as important factors for tissue-specific pathology in this disease.

interferon lambda | lupus | autoimmunity | skin | inflammation

Systemic lupus erythematosus (SLE) is a complex autoimmune syndrome that can affect multiple organs, including the skin and kidneys (1). Type I interferons (IFNs) are central to the pathogenesis of SLE and to its associated organ damage. These antiviral cytokines are induced by various danger signals, including activation of toll-like receptors (TLRs) during acute viral infections. Type I IFNs are also chronically elevated in a number of systemic autoimmune diseases, including SLE (2). Patients with SLE have a characteristic IFN signature with increased expression of IFN-stimulated genes (ISGs) in peripheral blood and affected tissues. Functionally, type I IFNs orchestrate a diverse network of inflammatory responses, such as renegade activation of myeloid cells and lymphocytes (3). Despite these findings, biologics targeting IFN-α or the type I IFN receptor (IFNAR1/2) have had mixed efficacy in clinical trials for human SLE, suggesting that other pathways may be additionally involved in lupus pathophysiology (4–7).

Recently, type III IFN lambdas (IFN-λs) have been identified as important mediators of immune responses at barrier surfaces (8–10). Four IFN-λ cytokines are expressed in human cells (IFN-λ1–4) and two are expressed in mouse cells (IFN-λ2/3). IFN-λs signal through a heterodimeric receptor complex composed of IFN-λ receptor 1 (IFNLR1) and IL-10 receptor 2 (IL-10R2) (11, 12). Although IFN-λs are structurally distinct from type I IFNs, they share important functional similarities and both utilize the JAK/STAT pathway to induce transcription of ISGs. One major difference between these two cytokine families is the expression profile of their receptor complex. The IFNAR is ubiquitous and expressed on almost all cell types. In contrast, IFNLR1 is more restricted and is highly expressed on epithelial cells (13). Recent evidence suggests that neutrophils and dendritic cell subsets may also respond to IFN-λ (14–16); however, it is unclear if these cytokines can directly activate other immune cells (17).

Because IFN-λs share functional properties with type I IFNs, it has been proposed that they may also contribute to autoimmunity (18). Indeed, several clinical reports have indicated that IFN-λ may be detrimental in SLE. One early study demonstrated that circulating IFN-λ1 is elevated in subjects with active SLE and correlates with disease activity, anti–double-stranded DNA (anti-dsDNA) autoantibodies, and glomerulonephritis (19). Another study reported that IFN-λ2/3 are also elevated in SLE serum and that lupus $CD4^+$ T cells express higher levels of *IFNL* transcripts relative to healthy controls (20). Moreover, genetic variants in the *IFNL* locus have recently been associated with increased risk for lupus in a Taiwanese cohort (21). IFN-λ cytokine has also been detected in skin and kidney biopsies of lupus patients with active disease, further suggesting that it may contribute to specific disease processes in these tissues (22, 23).

Despite these observations, the pathogenic effects of IFN-λ in autoimmune diseases remain somewhat controversial and are not well understood. Recent studies have even suggested that

Significance

Interferon lambdas share important functional similarities with type I interferons, but their role in inflammation and autoimmune disease remains controversial and has not been well studied. Here, we present evidence that interferon lambda is pathogenic and has nonredundant functions in TLR7-associated lupus inflammation. Most notably, we found that interferon lambda promotes systemic immune dysregulation through localized effects in the skin and kidneys. These data identify a role for interferon lambda in lupus immunobiology and tissue-specific pathology.

Author contributions: R.R.G., X.W., M.I.M., and M.J.K. designed research; R.R.G., X.W., L.J.O., S.N., K.H., L.P.B., M.I.M., and C.C.-R. performed research; J.B.K. and S.V.K. contributed new reagents/analytic tools; R.R.G., X.W., L.J.O., S.N., S.G., G.W., L.P.B., Z.-X.Y., and C.C.-R. analyzed data; R.R.G. and M.J.K. wrote the paper; and S.V.K. provided important scientific input.

The authors declare no competing interest.

This article is a PNAS Direct Submission.

Published under the PNAS license.

Data deposition: Single-cell RNA sequencing data have been deposited in the Gene Expression Omnibus (GEO) database (https://www.ncbi.nlm.nih.gov/geo/) under accession no. GSE142637.

[1]Present address: Department of Medicine, Perelman School of Medicine, University of Pennsylvania, Philadelphia, PA 19104.

[2]To whom correspondence may be addressed. Email: mariana.kaplan@nih.gov.

This article contains supporting information online at https://www.pnas.org/lookup/suppl/doi:10.1073/pnas.1916897117/-/DCSupplemental.

First published February 24, 2020.

IFN-λ can suppress inflammation by inhibiting neutrophil function in models of rheumatoid arthritis, colitis, and thromboinflammation (14, 16, 24). Given these conflicting results, additional mechanistic studies are necessary to fully investigate the role of IFN-λ in autoimmune pathology.

In our current study, we demonstrate that genetic deletion of IFNLR1 protects mice from immune dysregulation and organ damage in a model of TLR7-induced lupus. Furthermore, we demonstrate that keratinocytes and mesangial cells respond to IFN-λ and produce chemokines that promote inflammation in the skin and kidneys. These data provide compelling evidence that IFN-λ has important and nonredundant functions in the pathogenesis of lupus.

Results

IFN-λ Is Increased in TLR7-Induced Lupus and Promotes Systemic Immune Dysregulation. TLR7 activation induces expression of type I IFNs and is an important pathway in both murine and human lupus (Fig. 1*A*) (25–29). Healthy donor peripheral blood mononuclear cells (PBMCs) treated with the TLR7 agonist imiquimod (IMQ) also significantly up-regulated *IFNL1* transcripts (Fig. 1*A*), supporting the hypothesis that type III IFNs may also be involved in TLR7-associated autoimmune responses. To further investigate the potential contribution of IFN-λ in lupus autoimmunity, we treated wild-type (WT) and IFN-λ receptor-deficient (Ifnlr1$^{-/-}$) mice epicutaneously with IMQ for 5 wk (Fig. 1*B*). Mice treated with IMQ develop an autoimmune phenotype consistent with lupus, including increased type I IFN signature, leukocyte activation, specific autoantibodies, and other tissue pathologies in the skin, kidneys, and vasculature (30, 31). Notably, this model allowed us to study IFN-λ in lupus independently of confounding effects from murine susceptibility genes (such as the Fas mutation in the MRL/*lpr* strain) (32).

Consistent with the human PBMC data, IMQ-treated mice developed significantly higher concentrations of IFN-λ2/3 cytokine in serum relative to untreated mice (Fig. 1*C*). Immunofluorescent staining demonstrated that TLR7^{+} cells accumulate in the skin of IMQ-treated mice (Fig. 1*D*). qPCR also indicated that *TLR7* expression in skin was significantly increased in IMQ-treated mice, corroborating the tissue staining analysis (Fig. 1*E*). Moreover, these TLR7^{+} cells costained with Siglec H, a specific marker for plasmacytoid dendritic cells (pDCs, Fig. 1*D*). pDCs have been well characterized as an important source of type I IFN-α in both murine and human lupus (33). To further evaluate the role of pDCs, we purified pDCs and measured TLR7-induced IFN-λ production in culture supernatants. pDCs treated with IMQ for 24 h produced significantly higher amounts of IFN-λ protein compared to untreated controls (Fig. 1*F*). Together, these data indicated that pDCs may be a relevant source of IFN-λ production in the IMQ-induced lupus model.

As expected, WT mice treated with IMQ developed severe splenomegaly, calculated as percentage of spleen weight over body weight (Fig. 2*A*). WT + IMQ mice also developed leukocytosis, thrombocytopenia, and anemia (Fig. 2 *B–D* and *SI Appendix*, Fig. S1), further indicating systemic immune dysregulation and inflammation. In contrast, Ifnlr1$^{-/-}$ mice treated with IMQ had a significant reduction in splenomegaly and white blood cell counts, as well as improvements in circulating platelets and hemoglobin levels compared to WT + IMQ mice (Fig. 2 *A–D* and *SI*

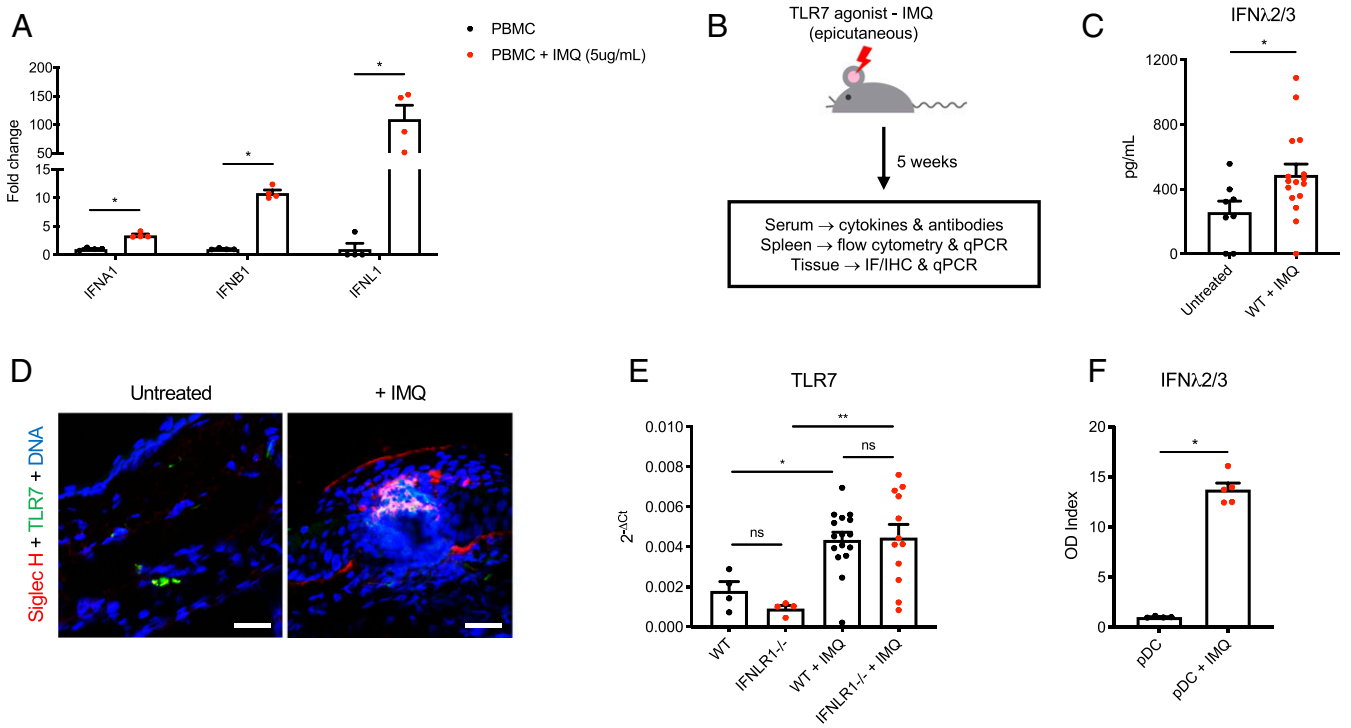

Fig. 1. IFN-λ is elevated in murine lupus. (*A*) IFN gene expression in healthy donor PBMCs. Cells were stimulated with the TLR7 agonist IMQ for 4 h and gene expression was quantified by qPCR ($n = 4$/group). (*B*) Schematic diagram of the IMQ-induced murine lupus model. (*C*) IFN-λ2/3 protein in murine lupus serum. Cytokine concentrations were measured by ELISA in mouse serum after 5 wk of IMQ treatment ($n = 8$ untreated, $n = 16$ treated). (*D*) Immunofluorescent staining for pDCs in murine lupus skin. TLR7 (green) and Siglec H (red) were detected in ear skin tissue after 5 wk of IMQ treatment. Tissue was counterstained with Hoechst (blue). (*E*) TLR7 expression in murine lupus skin. Gene expression was measured in ear tissue after 5 wk of IMQ treatment by qPCR ($n = 4$ WT, $n = 4$ Ifnlr1$^{-/-}$, $n = 16$ WT + IMQ, $n = 12$ Ifnlr1$^{-/-}$ + IMQ). (*F*) IFN-λ2/3 production by pDCs. Mouse pDCs were isolated from splenocytes by MACS column and treated with 5 μg/mL IMQ for 24 h ($n = 4$ untreated, $n = 5$ IMQ). IFN-λ2/3 protein was measured by ELISA in culture supernatants. Optical density (OD) values were blank corrected and normalized to untreated samples. Data are represented as mean ± SEM. Statistics were calculated by nonparametric Mann–Whitney *U* test or one-way ANOVA with Sidak correction for multiple comparisons. $^{*}P < 0.05$, $^{**}P < 0.01$; ns, not significant. (Scale bars in *D*: 25 μm.)

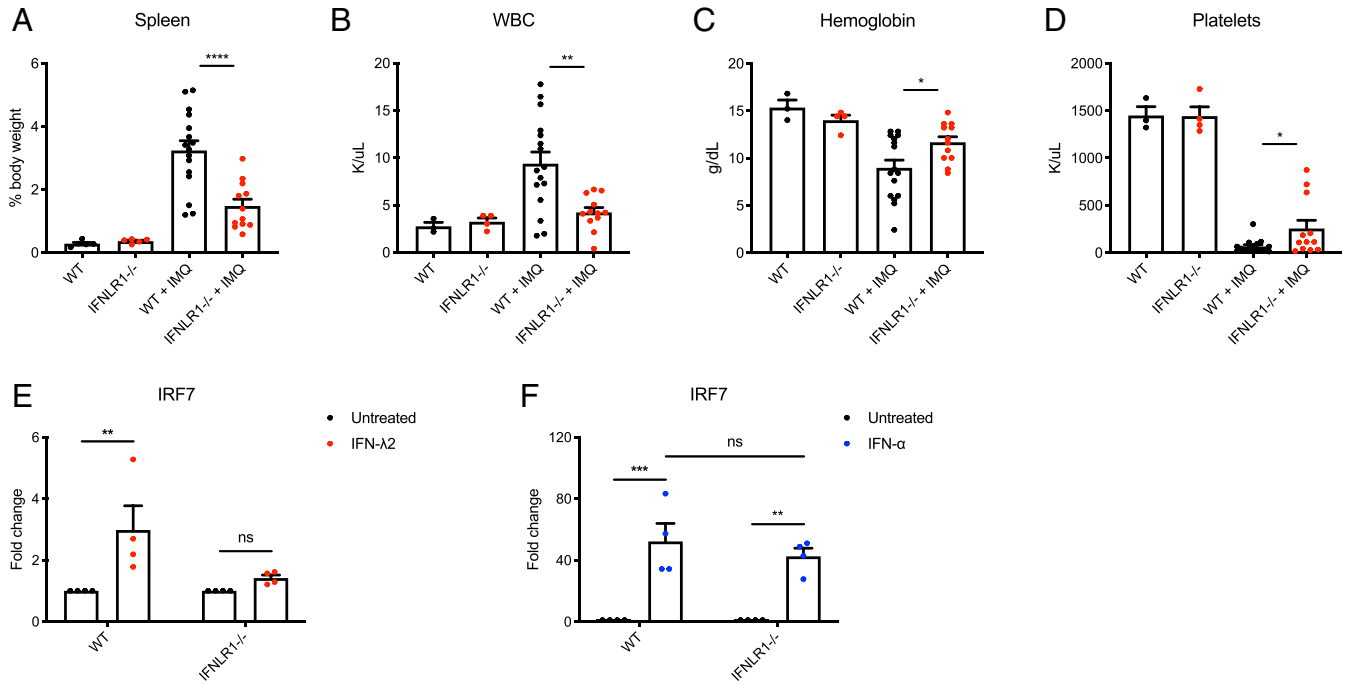

Fig. 2. IFN-λ promotes systemic immune dysregulation in murine lupus. (*A*) Splenomegaly in murine lupus. Spleens were collected after 5 wk of IMQ treatment and measured as percentage of total body weight ($n = 4$ WT, $n = 4$ Ifnlr1$^{-/-}$, $n = 16$ WT + IMQ, $n = 12$ Ifnlr1$^{-/-}$ + IMQ). (*B*) Leukocytosis, (*C*) anemia, and (*D*) thrombocytopenia in murine lupus. White blood cells (WBCs), hemoglobin, and platelets were quantified in peripheral blood after 5 wk of IMQ treatment ($n = 3$ WT, $n = 4$ Ifnlr1$^{-/-}$, $n = 16$ WT + IMQ, $n = 12$ Ifnlr1$^{-/-}$ + IMQ). (*E*) IFN-λ response and (*F*) IFN-α response in WT and Ifnlr1$^{-/-}$ mice. Splenocytes were stimulated with 100 ng/mL IFN-λ2 or 20 ng/mL IFN-α for 6 h. IRF7 expression was quantified by qPCR ($n = 4$/group). Data are represented as mean ± SEM. Statistics were calculated by nonparametric Mann–Whitney *U* test or two-way ANOVA with Sidak correction for multiple comparisons. *$P < 0.05$, **$P < 0.01$, ***$P < 0.001$, ****$P < 0.0001$; ns, not significant.

Appendix, Fig. S1). Splenocytes isolated from WT and Ifnlr1$^{-/-}$ mice had similar responses to stimulation with recombinant IFN-α, indicating that IFN-λ regulates inflammatory responses in TLR7-dependent lupus even in the presence of functional type I IFN pathways (Fig. 2*F*). No differences were observed in *TLR7* expression or *IFNA4* and *IFNB1* expression between WT and Ifnlr1$^{-/-}$ mice (Fig. 1*E* and *SI Appendix*, Fig. S2), suggesting that the upstream TLR7 pathway is also intact in Ifnlr1$^{-/-}$ mice. Finally, IFN-λ significantly induced *IRF7* expression in WT cells, but not Ifnlr1$^{-/-}$ cells, providing functional confirmation of the knockout model (Fig. 2*E*).

IFN-λ Promotes Myeloid Expansion and T Cell Activation but Is Not Required for B Cell Activation and Autoantibody Production. Given the differences in inflammatory responses between WT and Ifnlr1$^{-/-}$ mice treated with imiquimod, we further characterized the immune phenotype of these mice. Splenocytes were isolated at euthanasia and splenic immune cell populations were analyzed by multicolor flow cytometry. WT + IMQ mice had marked expansion of myeloid cells, including CD11b^{+} Ly6G^{+} neutrophils, CD11b^{+} Ly6C^{+} monocytes, and CD11b^{+} CD11c^{+} conventional DCs compared to untreated mice (Fig. 3 *A*–*C*, full gating strategies in *SI Appendix*, Fig. S3). WT + IMQ mice displayed increased levels of neutrophil extracellular traps (NETs) in serum and skin tissue (Fig. 3 *D* and *E*). WT + IMQ mice also had robust CD4^{+} and CD8^{+} T cell activation, with increased frequencies of T effector memory (CD62L^{-} CD44^{+}) cells and decreased frequencies of naïve T (CD62L^{+} CD44^{-}) cells (Fig. 3 *F*–*J*). Notably, Ifnlr1$^{-/-}$ + IMQ mice had significant reductions in myeloid cell expansion, NETs, and T cell activation compared to WT + IMQ mice (Fig. 3 *A*–*J*).

WT + IMQ mice also had increased frequencies of splenic CD138^{+} plasma B cells (Fig. 4*A*) and a corresponding decrease in IgM^{+} IgD^{+} naïve B cells (Fig. 4*B*) compared to untreated mice. In addition, WT + IMQ had increased surface expression of various B cell activation markers (Fig. 4 *C*–*E*) and increased levels of serum total IgG, anti-dsDNA, and antinuclear autoantibodies but no detectable anti-RNP (Fig. 4 *F*–*H* and *SI Appendix*, Fig. S4). In contrast to the changes observed for myeloid and T cells, Ifnlr1$^{-/-}$ + IMQ mice had no differences in splenic plasma cells, B cell activation markers, or serum autoantibodies compared to WT + IMQ mice (Fig. 4 *A* and *C*–*H* and *SI Appendix*, Fig. S4). These data indicate that IFN-λ has specific effects on immune dysregulation in TLR7-induced lupus, primarily in the myeloid and T cell compartments.

Immune Cells Are Not Broadly Responsive to IFN-λ. We next wondered whether the immune dysregulation observed in TLR7-dependent lupus resulted from direct effects of IFN-λ on immune effector cells. To systematically address this question, we utilized a high throughput single-cell RNA sequencing approach (34). Cells were isolated from WT mouse spleen and treated ex vivo with 100 ng/mL recombinant IFN-λ2 or recombinant IFN-α for 4 h. Cells were then captured for single-cell sequencing using the 10X Genomics platform. Uniform manifold approximation and projection (UMAP) clustering of mouse spleen cells revealed eight distinct immune cell populations, including the predominant lymphoid and myeloid cell types (Fig. 5*A* and *SI Appendix*, Fig. S5). Consistent with the literature, we found that *IFNAR1* was broadly expressed in immune cells, whereas *IFNLR1* was only detected at very low levels (*SI Appendix*, Fig. S6) (13, 35). To determine responsiveness of specific cell clusters to IFN-λ, we compared expression of core IFN-response genes. Mouse neutrophils, but not other immune cell clusters in spleen, significantly up-regulated ISGs following stimulation with IFN-λ

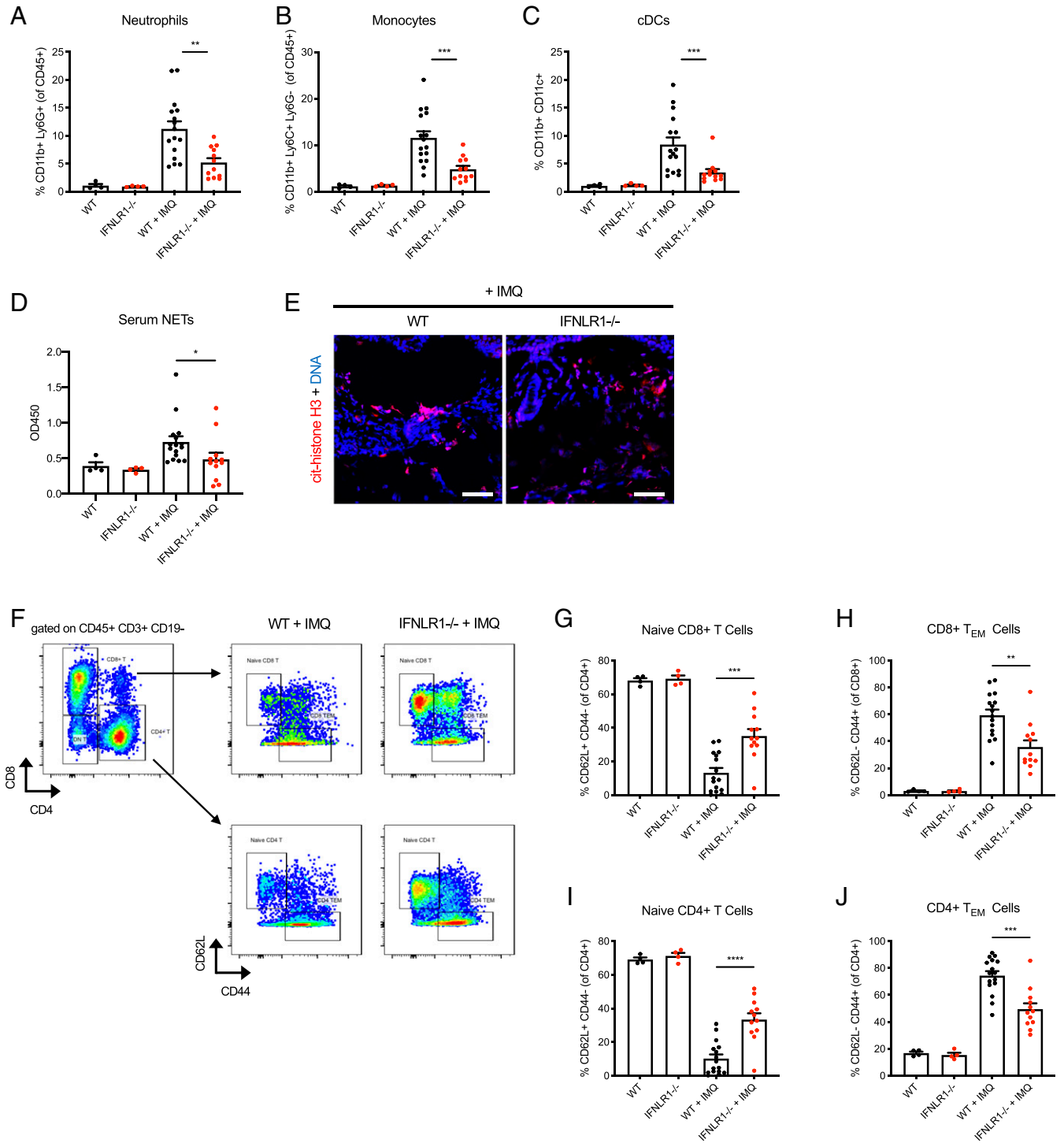

Fig. 3. IFN-λ promotes myeloid expansion and T cell activation. (*A*) Neutrophils, (*B*) monocytes, and (*C*) conventional dendritic cells in murine lupus. Cells were analyzed in spleen after 5 wk of IMQ treatment ($n = 4$ WT, $n = 4$ Ifnlr1$^{-/-}$, $n = 16$ WT + IMQ, $n = 12$ Ifnlr1$^{-/-}$ + IMQ). (*D*) NETs in serum and (*E*) skin tissue in murine lupus. NETs were detected in serum by ELISA for neutrophil elastase–DNA complexes. NETs were detected in ear skin tissue by immunofluorescent staining for citrullinated histone H3 (red) and DNA (Hoechst). (*F*) Representative gating strategy for T cell activation. (*G*) Naïve CD8$^+$, (*H*) CD8$^+$ effector memory, (*I*) naïve CD4, and (*J*) CD4$^+$ effector memory cells in murine lupus. T cell subsets were identified based on surface expression of CD62L and CD44 ($n = 4$ WT, $n = 4$ Ifnlr1$^{-/-}$, $n = 16$ WT + IMQ, $n = 12$ Ifnlr1$^{-/-}$ + IMQ). Data are represented as mean ± SEM. Statistics were calculated by nonparametric Mann–Whitney *U* test. **P* < 0.05, ***P* < 0.01, ****P* < 0.001, *****P* < 0.0001. (Scale bars in *E*: 50 μm.)

(Fig. 5*B*). In contrast, all immune cell types up-regulated ISGs following stimulation with IFN-α (Fig. 5*B*).

To investigate potential differences between mouse and human cells, we also performed an analogous single-cell RNA sequencing experiment on whole blood leukocytes isolated from a healthy human donor. Cells were treated with 100 ng/mL recombinant IFN-λ1 or recombinant IFN-α for 4 h and captured for sequencing. UMAP clustering identified eight different immune

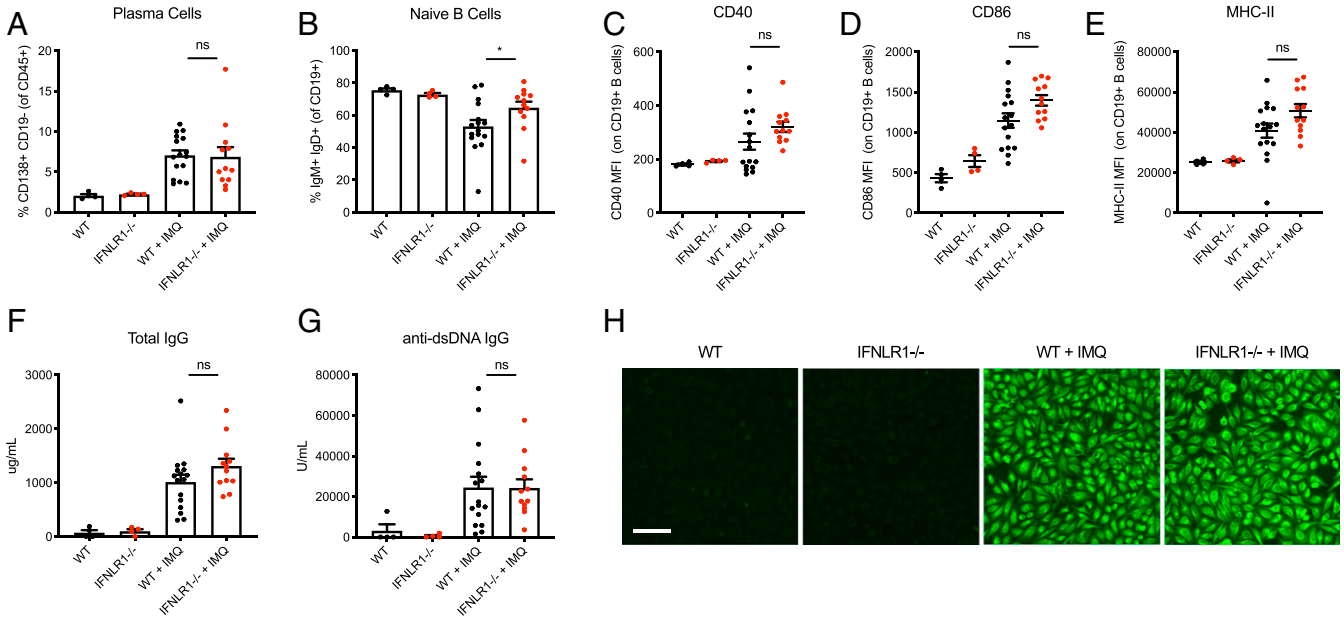

Fig. 4. IFN-λ is not required for B cell activation or autoantibody production. (*A*) Plasma cells and (*B*) naïve B cells in murine lupus. B cells were analyzed in spleen after 5 wk of IMQ treatment ($n = 4$ WT, $n = 4$ Ifnlr1$^{-/-}$, $n = 16$ WT + IMQ, $n = 12$ Ifnlr1$^{-/-}$ + IMQ). (*C–E*) Activation status of B cells in murine lupus. Mean fluorescent intensity of activation markers on CD19^{+} CD11b^{-} B cells ($n = 4$ WT, $n = 4$ Ifnlr1$^{-/-}$, $n = 16$ WT + IMQ, $n = 12$ Ifnlr1$^{-/-}$ + IMQ). (*F*) Total IgG, (*G*) anti-dsDNA IgG, and (*H*) antinuclear antibodies in murine lupus. Antibodies were quantified in mouse serum by ELISA or immunofluorescence on HEp-2 cells after 5 wk of IMQ treatment ($n = 4$ WT, $n = 4$ Ifnlr1$^{-/-}$, $n = 16$ WT + IMQ, $n = 12$ Ifnlr1$^{-/-}$ + IMQ). Data are represented as mean ± SEM. Statistics were calculated by nonparametric Mann–Whitney *U* test. *$P < 0.05$; ns, not significant. (Scale bar in *H*: 100 μm.)

cell populations in human peripheral blood (Fig. 5*C* and *SI Appendix*, Fig. S5). Similar to mouse samples, we found that immune cells broadly express *IFNAR1* but express *IFNLR1* only at very low levels (*SI Appendix*, Fig. S6). Human B cells, but not neutrophils or other immune cell clusters in peripheral blood, up-regulated ISGs following stimulation with IFN-λ (Fig. 5*D*). Again, all immune cell types responded to stimulation with IFN-α (Fig. 5*D*). To confirm these findings and determine if there are any differences between healthy controls and SLE patients, we isolated and treated B cells and neutrophils. Again, we found that human control and SLE B cells express higher levels of IFNLR1 and up-regulated ISGs in response to IFN-λ, whereas neutrophils did not respond (*SI Appendix*, Fig. S7). SLE leukocytes showed no differential response to IFN-λ compared to controls (*SI Appendix*, Fig. S7). These results indicated that only a narrow repertoire of immune cells respond to IFN-λ and that direct effects of IFN-λ are unlikely to explain the broad changes in immune phenotype associated with Ifnlr1 deficiency.

IFN-λ Promotes Skin Inflammation and Induces Chemokine Expression by Keratinocytes. Based on the single-cell analysis, we hypothesized that IFN-λ may orchestrate immune dysregulation and inflammation in lupus through localized effects at barrier sites, rather than direct effects on immune cells. Hematoxylin & eosin (H&E) staining of ear skin tissue revealed that WT + IMQ mice had a significant increase in immune cell infiltrates relative to untreated mice, including CD3^{+} T cells, CD19^{+} B cells, F4/80^{+} macrophages, and Ly6G^{+} neutrophils (Fig. 6 *A* and *B* and *SI Appendix*, Fig. S8). qPCR further demonstrated that WT + IMQ mice had increased expression of the IFN-λ receptor (*IFNLR1*) and proinflammatory cytokines/chemokines (*IL6*, *CXCL9*, *CXCL10*, *CXCL11*) in ear skin tissue over untreated controls (*SI Appendix*, Fig. S9 and Fig. 6 *C–F*). Ifnlr1$^{-/-}$ + IMQ mice had significant decreases in skin inflammation and skin cytokine/chemokine expression compared to WT + IMQ mice (Fig. 6 *A–F*). ISGs were also increased in skin tissue of WT + IMQ mice relative to untreated controls; however, no differences were observed in skin ISGs between WT + IMQ and Ifnlr1$^{-/-}$ + IMQ mice (*SI Appendix*, Fig. S10).

Given these data, we next hypothesized that structural cells in the skin may be key responders to IFN-λ and coordinate immune responses through expression of proinflammatory chemokines. Keratinocytes are the most abundant cell type in the skin and have been implicated in the pathogenesis of SLE and other inflammatory skin diseases (36, 37). Previous reports have indicated that keratinocytes express the IFNLR and respond to stimulation with IFN-λ cytokine (11, 22, 38). Confirming these reports, we found that primary mouse keratinocytes isolated from WT neonatal skin responded to stimulation with recombinant IFN-λ2 and significantly up-regulated ISGs (Fig. 7*A*). Ifnlr1$^{-/-}$ keratinocytes did not respond to stimulation with IFN-λ2, indicating the specificity of this effect (Fig. 7*A*). We further observed that HaCaT human epidermal keratinocytes respond similarly to IFN-λ1 and up-regulate ISGs (Fig. 7 *B* and *C*). Notably, the kinetics of ISG induction appeared to differ between IFN-λ and IFN-α, with IFN-λ inducing more sustained responses at later timepoints. IFN-λ also induced significant expression of *CXCL10* and *CXCL11* chemokines in HaCaT keratinocytes (Fig. 7 *E* and *F*) and moderate expression of *CXCL9* (Fig. 7*D*). These results are consistent with the decrease in skin chemokine expression between WT + IMQ and Ifnlr1$^{-/-}$ + IMQ mice (Fig. 6 *C–F*).

As expected, IFN-α induced significant expression of *CXCL9*, *CXCL10*, and *CXCL11* (Fig. 7 *D–F*). Notably, keratinocytes treated with both IFN-λ and IFN-α had significantly higher chemokine expression relative to either cytokine alone, indicating that type I and type III IFNs have additive effects on chemokine expression (*SI Appendix*, Fig. S11). IFN-λ and IFN-α also induced *IL6* transcripts and MHC-I surface expression by keratinocytes at similar levels but did not induce *IL8* or MHC-II (*SI Appendix*, Fig. S12). We also assessed if keratinocytes themselves could be a potential source of IFN-λ in response to TLR7 activation. IMQ did not induce expression of *IFNL1*

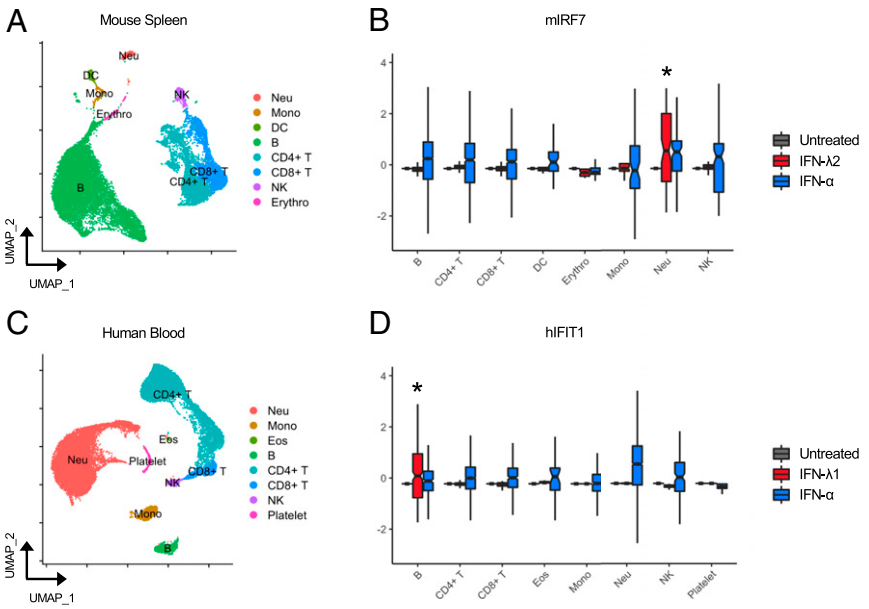

Fig. 5. Immune cells are selectively responsive to IFN-λ. (*A*) UMAP clustering of WT mouse spleen cells treated with 100 ng/mL of IFN-λ2 or IFN-α for 4 h (n = 18,520 cells). (*B*) IFN-stimulated gene expression in untreated and IFN-treated mouse cell clusters. (*C*) UMAP clustering of human whole blood cells treated with 100 ng/mL of IFN-λ1 or IFN-α for 4 h (n = 19,266 cells). (*D*) IFN-stimulated gene expression in untreated and IFN-treated human cell clusters. Data are represented as notched boxplots (median with interquartile range; notch represents 95% confidence interval of the median). Statistics were calculated by one-way ANOVA with Tukey's honest significant differences. *P < 0.005.

by HaCaT keratinocytes. Of note, keratinocytes treated with recombinant IFN-α up-regulated expression of *IFNL* transcripts, suggesting that type I IFNs may secondarily contribute to local production of IFN-λs in skin (*SI Appendix*, Fig. S13).

To further investigate the functional relevance of IFN-λ–induced chemokines, we performed a Transwell migration assay. Human keratinocytes were treated in vitro with recombinant IFN-λ or IFN-α and cell-free culture supernatants were collected after 48 h. Keratinocyte-conditioned media were added to the bottom chamber of a Transwell insert. Healthy donor human PBMCs were then added into the top chamber of the Transwell and incubated for 24 h to quantify cell migration toward the keratinocyte-conditioned media. Cells that migrated into the bottom chamber were collected after 24 h and analyzed by flow cytometry. Supernatants from keratinocytes treated with IFN-λ or IFN-α induced significant migration of PBMCs (Fig. 7*G*). Further investigation revealed that IFN-λ induced significant migration of $CD14^+$ monocytes, B cells, and T cells. In contrast, IFN-α preferentially induced migration of natural killer (NK) cells and T cells, but not monocytes (*SI Appendix*, Fig. S14). Overall, these results indicated that IFN-λ induces skin inflammation in lupus through chemokine expression by keratinocytes and that IFN-λ may have unique effects on migration of specific cell subsets.

IFN-λ Promotes Lupus-Associated Renal Pathology and Activates Mesangial Cells. In addition to skin inflammation, we also explored the possible effects of IFN-λ in other lupus-associated tissue pathologies. In particular, SLE can target the kidneys and cause irreversible renal damage. Consistent with previous reports, immunofluorescent microscopy demonstrated that WT + IMQ mice developed significant immune complex deposition in glomeruli (Fig. 8 *A*–*C*) (30, 31). Periodic acid-Schiff (PAS) staining also revealed that WT + IMQ mice developed glomerulosclerosis and increased mesangial matrix (Fig. 8 *D* and *E*). These effects were significantly reduced in $Ifnlr1^{-/-}$ + IMQ mice (Fig. 8 *A*–*E*).

To further investigate the molecular effects of IFN-λ in kidney disease, we performed qPCR on kidney tissue to measure gene expression in situ. Kidneys from WT + IMQ mice had increased expression of various ISGs (*MX1*, *IRF7*, *ISG15*, *RSAD2*) relative to untreated mice (Fig. 8*F*). These ISGs were significantly reduced in $Ifnlr1^{-/-}$ + IMQ mice (Fig. 8*F*). To address whether IFN-λ may activate structural cells within the kidney, we treated Mes13 mouse mesangial cells with IFNs. Similar to keratinocytes, Mes13 cells treated with IFN-λ or IFN-α significantly up-regulated ISGs (Fig. 8 *G* and *H* and *SI Appendix*, Fig. S15), as well as the chemokine genes *CXCL9*, *CXCL10*, and *CXCL11* (Fig. 8 *I*–*K*). These results further indicated that type III IFNs can directly activate structural cells in tissues and represent a parallel mechanism that may be involved in lupus-associated renal damage.

Finally, we explored the possible effects of IFN-λ on lupus-associated vascular disease. As described previously, WT + IMQ mice developed significant impairments in endothelium-dependent vasorelaxation compared to untreated controls in a myograph assay (*SI Appendix*, Fig. S16) (31). This phenomenon has previously been reported to be dependent on type I IFNs and plays an important role in lupus vasculopathy, as well as in progression to atherosclerosis and overt vascular disease (39). Unlike the improvements seen in skin and kidney, $Ifnlr1^{-/-}$ + IMQ mice had similar levels of vascular dysfunction as WT + IMQ mice, suggesting that type I and type III IFNs have distinct, tissue-specific effects in lupus autoimmunity and associated organ damage.

Discussion

IFN-λs are critical factors in immune defense at barrier surfaces. While recent studies have also indicated that these cytokines are elevated in human SLE, their role in immune dysregulation and autoimmunity remains controversial and has not been systematically defined. In this study, we provide evidence that IFN-λ has distinct pathogenic roles in immune dysregulation and tissue inflammation in lupus. We found that exposure to danger signals such as TLR7 agonists increases serum IFN-λ cytokine levels in murine lupus, likely through effects on pDCs. Moreover, Ifnlr1-deficient mice are protected from several features characteristic

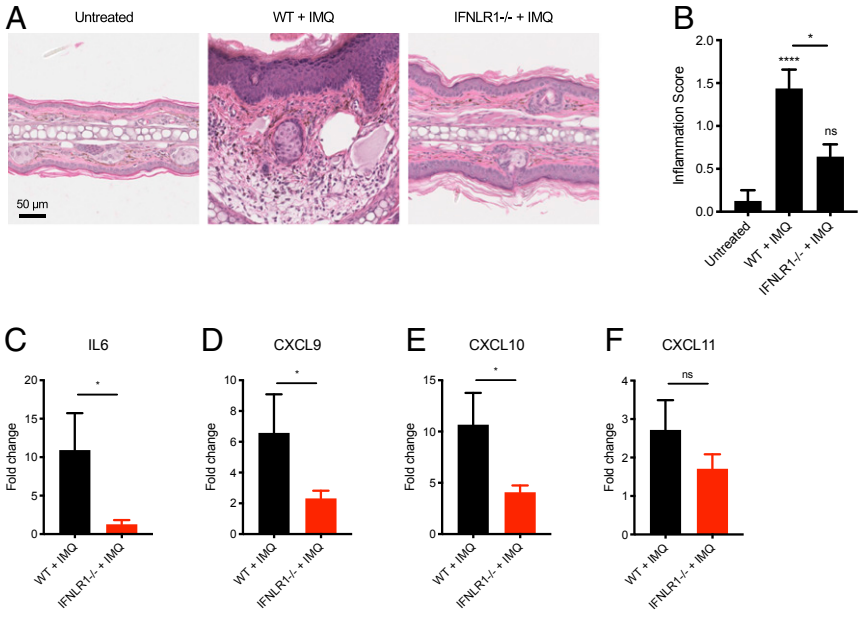

Fig. 6. IFN-λ promotes skin inflammation. (*A*) H&E staining and (*B*) pathology scoring of ear skin in murine lupus. Tissue sections were prepared after 5 wk of IMQ treatment ($n = 8$ untreated, $n = 8$ WT + IMQ, $n = 7$ Ifnlr1$^{-/-}$ + IMQ). (*C–F*) Inflammatory cytokine and chemokine expression in murine lupus skin. Gene expression was measured in ear tissue after 5 wk of IMQ treatment by qPCR ($n = 8$ untreated, $n = 16$ WT + IMQ, $n = 12$ Ifnlr1$^{-/-}$ + IMQ). Data were normalized to untreated mice. Data are represented as mean ± SEM. Statistics were calculated by one-way ANOVA with Tukey's correction for multiple comparisons or nonparametric Mann–Whitney *U* test. *$P < 0.05$, ****$P < 0.0001$; ns, not significant.

of lupus immune dysregulation, including myeloid expansion and T cell activation. Ifnlr1-deficient mice were also protected from clinical and histopathologic manifestations of lupus, such as anemia, thrombocytopenia, skin and kidney inflammation, and immune complex deposition. Notably, Ifnlr1$^{-/-}$ mice had intact responses to type I IFNs, suggesting that IFN-λs have important and nonredundant functions in lupus-associated pathology.

In contrast to IFN-α, IFN-λ activity is most potent at epithelial barriers (40). Previous data indicate that some immune cells, including dendritic cells and neutrophils, express the IFNLR; however, these studies did not investigate responses across different immune cell populations and data in human samples are especially lacking (17). To address whether IFN-λ has direct effects on immune cell function, we performed single-cell RNA sequencing on leukocytes stimulated with IFN-λ. This approach allowed us to evaluate IFN response in multiple cell populations without using density gradients, cell sorting, or cell selection kits that may lead to activation. Confirming previous reports, we found that mouse neutrophils residing in spleen respond to IFN-λ and up-regulate canonical ISGs (14, 41). However, we could not reproduce this finding in human peripheral blood neutrophils. These data partially contradict previous consensus that neutrophils are the primary immune cell type that respond to IFN-λ (40). One recent study demonstrated that human neutrophils express IFNLR1 transcripts; however the study did not measure functional readouts of IFN-λ signaling such as induction of ISGs (41). We also found that human peripheral blood B cells (but not mouse B cells in the spleen) respond to IFN-λ. These findings are consistent with a previous report that IFN-λ increases TLR7-mediated antibody production in human B cells (42). Although we did not detect any effects of IFN-λ on B cell activation or autoantibodies in our model of murine lupus, it is possible that IFN-λ directly modulates B cell responses in human SLE. Such differences between mouse and human cells merit further investigation and are an important consideration for future studies on the effects of type III interferons in infection or autoimmunity. Together, our data demonstrate that only a narrow repertoire of immune cells is responsive to IFN-λ and direct effects on these cells are unlikely to explain the systemic immune dysregulation observed in our model.

Based on these data, we hypothesized that IFN-λ may instead promote immune dysregulation through localized effects at barrier surfaces such as the skin. *IFNLR1* expression was increased in murine lupus skin and Ifnlr1-deficient mice had significant reductions in TLR7-induced skin inflammation. Further investigation revealed that Ifnlr1$^{-/-}$ mice had lower expression of proinflammatory cytokines and chemokines (*IL6*, *CXCL9*, *CXCL10*) in skin tissue. Keratinocytes are the most abundant cell type in skin and have been implicated in SLE and a variety of other inflammatory skin diseases (36, 37). Previous reports suggest that keratinocytes respond to IFN-λ in vitro (11, 38). IFN-λ cytokine has also been detected in skin lesions of patients with cutaneous lupus and colocalizes with IFN-inducible proteins (22). Building on these reports, we found that keratinocytes directly respond to IFN-λ stimulation and produce proinflammatory molecules that induce migration of monocytes and lymphocytes. In particular, keratinocytes treated with IFN-λ upregulate chemokines that bind to the chemokine receptor CXCR3 and promote immune cell recruitment to sites of inflammation. CXCR3 and its associated chemokines (CXCL9, CXCL10, CXCL11) have been closely associated with lupus autoimmunity. CXCR3^{+} cells are increased in skin and kidney of SLE subjects and colocalize with CXCL10-producing cells (43, 44). Moreover, CXCR3$^{-/-}$ mice are protected from lupus nephritis in the MRL/*lpr* mouse model (45). IFN-λ also increased MHC-I expression by keratinocytes and may be involved in potentiating CD8^{+} T cell responses. Overall, these observations provide evidence that type III IFNs promote skin inflammation through effects on keratinocytes, leading to expression of chemokines and immunostimulatory molecules that induce immune cell recruitment and clinical skin disease in lupus. Our results further suggest that keratinocytes may have distinct responses to type I and type III IFNs, especially in their ability to recruit specific cell subsets.

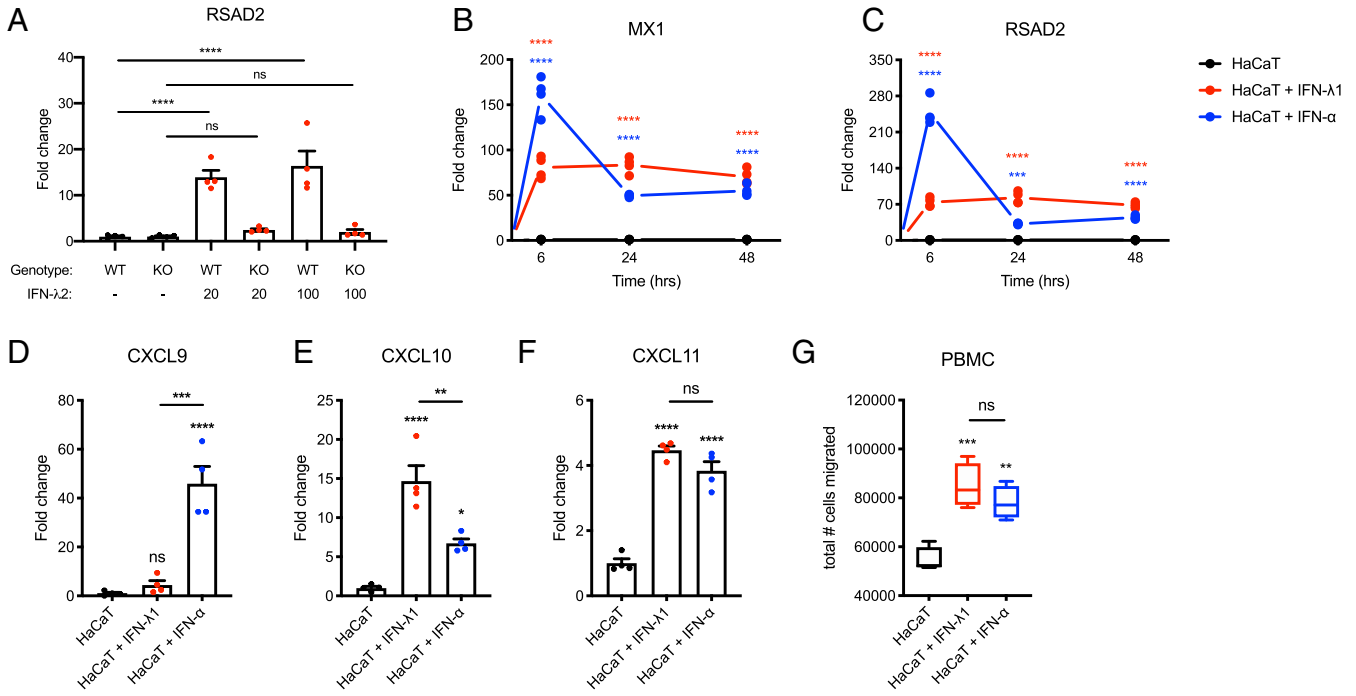

Fig. 7. IFN-λ induces chemokine expression and immune cell recruitment by keratinocytes. (*A*) Primary murine keratinocytes were isolated from neonate mice and treated with IFN-λ2 at the indicated concentrations (ng/mL) for 6 h. RSAD2 gene expression was measured by qPCR ($n = 4$/group). (*B* and *C*) HaCaT keratinocytes were treated with 20 ng/mL of IFN-λ1 or IFN-α. IFN-stimulated gene expression was measured at the indicated timepoints by qPCR ($n = 4$/group). (*D–F*) CXCL chemokine gene expression in HaCaT cells after 24 h of stimulation with IFN-λ1 or IFN-α ($n = 4$/group). (*G*) PBMC migration assay: 500,000 healthy donor PBMCs were seeded in the top chamber of a Transwell (*Inset*) and incubated with culture supernatants from keratinocytes treated with IFN for 48 h ($n = 4$/group). Cells migrated into the bottom chamber were counted after 24 h in the Transwell culture. Data are represented as mean ± SEM or median ± min/max (boxplots). Statistics were calculated by one-way ANOVA with Tukey's correction for multiple comparisons. $*P < 0.05$, $**P < 0.01$, $***P < 0.001$, $****P < 0.0001$.

In addition, we found that IFN-λ and IFN-α have additive effects on chemokine expression by keratinocytes. This likely represents the tissue microenvironment in vivo, where keratinocytes are exposed to an array of different cytokines, including both IFN-λ and IFN-α. Interestingly, IFN-α also induced IFN-λ expression by keratinocytes, suggesting that type I IFNs can integrate with and amplify type III IFN responses at barrier surfaces. These data support previous reports that IFN-α primes IFN-λ production and that IFNAR$^{-/-}$ mice have defective production of IFN-λ in response to *Aspergillus* infection (41, 46). Consistent with a previous study, we found that keratinocytes do not respond to TLR7 agonists, indicating that, unlike pDCs, they are not a primary source of IFN-λ (or IFN-α) in TLR7-induced inflammatory responses (47). However, this secondary mechanism of IFN-α–mediated IFN-λ production may be important in the context of lupus autoimmunity, where existing type I IFN responses could further induce type III IFNs in a vicious cycle that worsens inflammation and tissue damage.

Our study also investigated the effects of IFN-λ on other types of lupus-associated tissue pathology. We observed significant reductions in several histologic parameters of kidney disease, including immune complex deposition and glomerulosclerosis. Within the kidney, we identified that mesangial cells directly respond to IFN-λ, up-regulating expression of ISGs and CXCL chemokines. This represents an analogous mechanism to that seen in keratinocytes in the skin and could contribute to renal inflammation, glomerulonephritis, and progressive kidney damage. Indeed, these data support previous studies indicating that IFN-λ protein is expressed in renal biopsies and serum IFN-λ levels correlate with glomerulonephritis in patients with SLE (19, 23). Although Ifnlr1 deficiency protected mice from lupus-associated renal manifestations, it did not improve systemic vasculopathy, supporting the concept that IFN-λ modulates skin and renal disease through distinct tissue-specific effects.

Although our data provide several independent lines of evidence that IFN-λ promotes tissue inflammation, there are some limitations in our study. It is possible that IFN-λ induces expression of other cytokines and immunostimulatory molecules beyond those measured in our experiments. Further experiments are necessary to fully investigate how type III IFNs affect keratinocyte or mesangial cell function and how these responses may differ from type I IFNs. Moreover, it is possible that other cells in tissue, including Langerhans cells and melanocytes, can respond to IFN-λ and drive immune responses (38). It has also been proposed that IFN-λ fails to induce proinflammatory responses in comparison to IFN-α due to insufficient activation of IRF1 (48). While this threshold effect may prevent tissue damage during acute infections (where IFN-λ expression is more transient), our data suggest that IFN-λ is capable of inducing a proinflammatory program in epithelial cells in the context of chronic IFN production. Regardless, it is necessary to corroborate the effects of IFN-λ in other lupus models. Although the TLR7–IFN axis is an important mechanism in SLE, it is not the only pathway involved in the complex etiology of lupus autoimmunity.

Importantly, our findings challenge some existing paradigms in lupus immunobiology. Since it is not currently possible to distinguish between the transcriptional profiles of IFN-α and IFN-λ, it is likely that IFN-λ has been underappreciated as a pathogenic factor in SLE (49). As such, the contributions of IFN-λ to lupus pathogenesis may partially explain why drugs targeting only IFN-α or type I IFN receptor have had mixed responses that fall short of the therapeutic benefits predicted by the existing literature (3). New treatment strategies that target

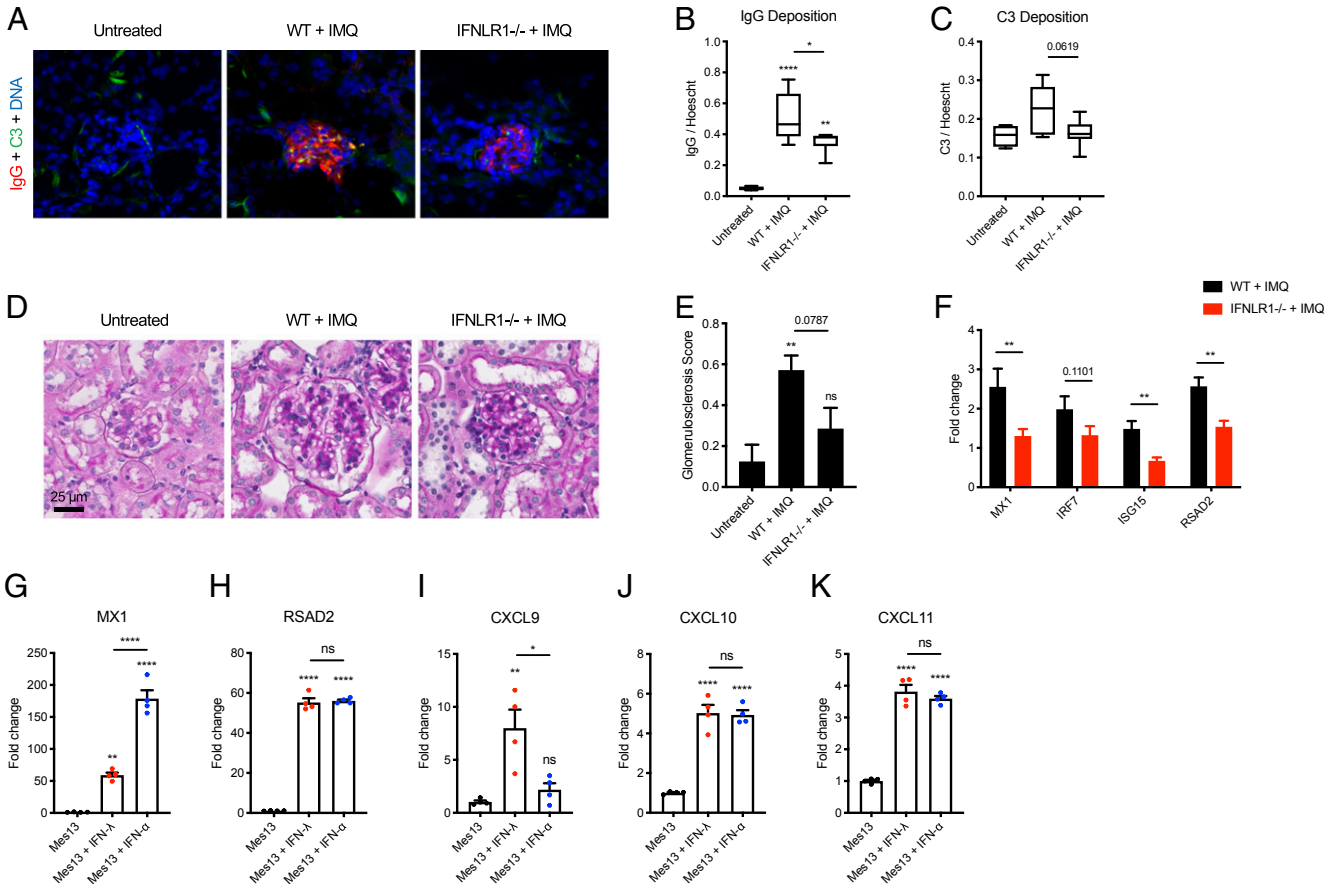

Fig. 8. IFN-λ promotes lupus-associated renal pathology and activates mesangial cells. (*A*) Immunofluorescent staining for immune complex deposition in murine lupus kidneys. Renal tissue was prepared after 5 wk of IMQ treatment. (*B*) IgG and (*C*) C3 deposition were quantified as fluorescent intensity within individual glomeruli and normalized to Hoechst staining. A total of 10 to 15 glomeruli were scored for each mouse and averaged ($n = 4$ untreated, $n = 8$ WT + IMQ, $n = 7$ Ifnlr1$^{-/-}$ + IMQ). (*D*) PAS staining and (*E*) pathology scoring of murine lupus kidney sections ($n = 8$ untreated, $n = 7$ WT + IMQ, $n = 7$ Ifnlr1$^{-/-}$ + IMQ). (*F*) IFN-stimulated gene expression in kidney tissue. Gene expression was determined by qPCR and normalized to untreated mice ($n = 8$ untreated, $n = 16$ WT + IMQ, $n = 12$ Ifnlr1$^{-/-}$ + IMQ). (*G* and *H*) IFN-stimulated gene expression and (*I*–*K*) CXCL chemokine expression in cultured mouse Mes13 mesangial cells. Mes13 cells were treated with 20 ng/mL IFN-λ2 or IFN-α for 24 h ($n = 4$/group) and gene expression was determined by qPCR. Data are represented as mean ± SEM or median + min/max (boxplots). Statistics were calculated by one-way ANOVA with Tukey's correction for multiple comparisons or nonparametric Mann–Whitney *U* test. **P* < 0.05, ***P* < 0.01, *****P* < 0.0001; ns, not significant.

shared elements of type I and type III interferons, such as the downstream JAK/STAT signaling cascade, may therefore be a more effective approach for patients with SLE (50, 51).

In summary, we propose that IFN-λ has nonredundant functions in TLR7-dependent lupus and regulates tissue inflammation through specific effects on skin and kidney cells. These tissue-specific effects may subsequently lead to systemic immune dysregulation. Our data offer insights into the molecular pathogenesis of lupus and could have broad implications for basic and translational understanding of autoimmune diseases.

Methods

Mice. WT C57BL/6 mice were purchased from The Jackson Laboratory. Ifnlr1$^{-/-}$ mice were generated as previously described (52). Mice were bred under specific pathogen-free conditions and all experiments were done in accordance with NIH guidelines under the NIAMS animal protocol A016-05-26.

IMQ Model. Eight- to 10-wk-old WT or Ifnlr1$^{-/-}$ mice were treated with imiquimod as described previously to induce a lupus-like phenotype (30). A 5% imiquimod cream (Fougera Pharmaceuticals) was applied topically to the inner ear three times a week for 5 wk. Mice were killed 48 to 72 h after the final treatment. Blood was collected by terminal cardiac puncture. Ears and kidneys were harvested for RNA, protein, and histology. Spleens were isolated and smashed through a 70 μM sterile filter to obtain single-cell suspensions. Red blood cells (RBCs) were lysed using ammonium–chloride–potassium (ACK) lysing buffer.

RNA Extraction, cDNA Synthesis, and qPCR. RNA was extracted from cells or tissue using TRIzol reagent (Thermo Fisher). Skin and kidney tissues were frozen with liquid nitrogen and ground into a fine powder using a mortar and pestle prior to RNA extraction. RNA was purified using Direct-zol RNA kits (Zymo Research) and quantified with a Nanodrop spectrophotometer. A total of 200 ng RNA was used for cDNA synthesis with iScript reverse transcription supermix (Bio-Rad). Quantitative real-time PCR was performed on a CFX96 real-time PCR detection system (Bio-Rad) using TaqMan gene expression master mix and specific probes (Thermo Fisher). All TaqMan assay IDs are listed in *SI Appendix*, Table S1. Expression values were normalized to *gapdh* as an internal housekeeping gene and fold change was calculated using the ΔΔCt method.

Flow Cytometry. Cells were stained in FACS buffer (phosphate-buffered saline [PBS] + 2% fetal bovine serum [FBS]). Briefly, cells were incubated with 100 μL TruStain FcX on ice for 10 min. After Fc block, 50 μL antibody master mix was added and cells were incubated on ice for 30 min (protected from light). Cells were subsequently washed with FACS buffer and fixed with 2% PFA. Cells were washed again and resuspended in FACS buffer. Samples were acquired on a BD LSR-Fortessa or BD FACSCanto. Data were analyzed using FlowJo software. Gating strategies are indicated in the supplemental figures. All FACS antibodies and dilutions are listed in *SI Appendix*, Table S2.

Detection of Cytokines, NETs, and Autoantibodies. Serum was separated from whole blood using Z-Gel tubes (Sarstedt). Mouse IFN lambda 2/3 cytokine was measured in mouse serum and pDC culture supernatant by DuoSet ELISA kit according to the manufacturer's instructions (R&D Systems). NETs were quantified in serum by custom ELISA. Briefly, plates were coated with anti-human neutrophil elastase antibody (EMD Millipore 481001, 1:2,000 dilution) overnight. Plates were blocked with 1% bovine serum albumin (BSA). Mouse serum was diluted 1:50 in 1% BSA and incubated overnight at 4 °C. Plate were washed and subsequently incubated with anti-mouse dsDNA antibody (EMD Millipore MAB030, 1:100 dilution). Plates were washed again and incubated with anti-mouse HRP-conjugated secondary antibody (Bio-Rad 1706516). TMB substrate and Stop Solution (Thermo Fisher) were used for colorimetric detection. Total IgG, anti-dsDNA IgG, and anti-RNP Ig were also quantified in mouse serum by ELISA according to the manufacturer's instructions (Thermo Fisher and Alpha Diagnostics, respectively). Antinuclear antibodies were determined by immunofluorescence (1:40 serum dilution) on HEp-2 antigen substrate slides according to the manufacturer's instructions (MBL International).

Histology and Immunofluorescence. Skin and kidney samples were fixed in 10% formalin solution overnight and transferred to 70% EtOH. Tissues were paraffin embedded and prepared for H&E and PAS staining by the Pathology Core Facility, National Heart, Lung, and Blood Institute. Histopathology slides were digitally scanned and analyzed using NDP.viewer 2.0 software (Hamamatsu). Slides were scored based on histopathological criteria. Pathologists were blinded to the genetic background and treatment group for all samples. CD3, CD19, F4/80, and Ly6G were detected in skin tissue by immunohistochemistry. Frozen issues were also prepared for immunofluorescent staining. For immunofluorescent detection of pDCs and NETs, skin was snap frozen in OCT compound (Tissue-Tek). For immunofluorescent detection of immune complex deposition, kidneys were perfused with PBS and snap frozen in OCT. Frozen sections were fixed in cold acetone for 10 min and washed with PBS. Slides were blocked with 5% sterile-filtered BSA overnight at 4 °C and incubated with antibodies diluted in 1% BSA. Samples were washed with PBS and counterstained with 1:1,000 Hoechst. Slides were sealed using Prolong Gold. All images were captured on a Zeiss LSM780 confocal microscope using the same acquisition settings. IgG and C3 were quantified by fluorescence intensity and measured in 10 to 15 independent glomeruli for each mouse using Fiji software. IgG and C3 intensity were subsequently normalized to Hoechst intensity within the same glomerulus to calculate a deposition metric. All antibodies are listed in *SI Appendix*, Table S2.

Single-Cell RNA-Seq. Mouse splenocytes were isolated as described above. RBCs were lysed with ACK buffer. For human samples, cells were isolated from whole blood of healthy volunteers using ErythroClear RBC depletion kit (STEMCELL). Cells were resuspended in RPMI supplemented with 10% FBS and 1% penicillin/streptomycin (Pen/Strep) and treated with 100 ng/mL recombinant IFN-λ/IFN-α for 4 h. Single cells were sequenced using the 10X Genomics platform. Cells were encapsulated using microfluidics technology and barcoded using a unique molecular identifier. cDNA was prepared according to the manufacturer's instructions and sequenced on an Illumina 3000 HiSeq system. Data were demultiplexed using Cell Ranger software to generate fastq files. Data were then aligned to the mouse or human reference genome using STAR. Cell Ranger output files were loaded into R for analysis using the Seurat package (53). Low-quality cells were removed based on percent mitochondrial gene expression. Data were integrated, normalized, and transformed for downstream analysis. Clustering was performed using the UMAP algorithm. Cell clusters were annotated using the SingleR algorithm (54). Unclassified cells were removed from downstream analysis. Gene expression was subsequently determined in each cluster. Data were visualized using ggplot2.

Cell Isolation and Culture. Peripheral blood was collected from healthy volunteers or SLE subjects by venipuncture at the NIH Clinical Center. Patients signed informed consent and all experiments involving human subjects were approved by the NIAMS Institutional Review Board (NIH 94-AR-0066). Peripheral blood mononuclear cells were isolated using Ficoll-Paque density gradient (GE Life Sciences). B cells were subsequently isolated from PBMCs using an EasySep kit (STEMCELL). Neutrophils were isolated by dextran sedimentation. Red blood cells were lysed using hypotonic 0.2 NaCl followed by 1.8% NaCl. Cells were then resuspended in RPMI supplemented with 10% FBS and 1% Pen/Strep and treated as indicated.

pDCs were isolated from mouse splenocytes using a MACS isolation kit (Miltenyi Biotec) and cultured in RPMI supplemented with 10% FBS and 1% Pen/Strep. Primary keratinocytes were isolated from neonate mice as previously described (55, 56) and were cultured in low calcium medium (8% chelated FCS, 0.05 mM Ca^{2+}). Cells were plated in 12-well plates (2×10^5 cells/well) and treated with recombinant IFNs as indicated. HaCaT human keratinocytes were obtained from AddexBio and cultured in Dulbecco's modified Eagle medium (DMEM) supplemented with 10% FBS and 1% Pen/Strep. Mes13 mouse mesangial cells were cultured in DMEM/F12 supplemented with 5% FBS and 1% Pen/Strep. Adherent cells were detached using 0.25% trypsin-EDTA solution and plated in 12- or 24-well plates for stimulation with TLR agonists or recombinant cytokines. All chemical reagents and recombinant proteins used in the study are listed in *SI Appendix*, Table S3.

Transwell Migration Assay. In vitro migration assays were performed using polycarbonate Transwell inserts (Corning, 5-μm pore size). Healthy donor PBMCs were resuspended in keratinocyte media and 500,000 cells were added to the top chamber of each insert. A total of 500 μl keratinocyte-conditioned culture media was subsequently added to the lower chamber. Cells that migrated into the bottom chamber were collected after 24 h. Adherent cells were detached using 0.25% trypsin-EDTA solution. Cells were counted with a hemocytometer and stained for FACS analysis with lymphocyte and monocyte markers as described above.

Endothelium-Dependent Vasorelaxation Assays. Murine aortic rings (~2 mm) were excised and mounted in a myograph system (Danish Myo Technology A/S) containing physiological salt solution (PSS) with aeration (95% O2/5% CO_2). Aortas were stabilized in PSS with 700 mg passive pressure and equilibrated for 1 h. Contraction was achieved with PSS containing 100 mM potassium chloride (KPSS) prior to collecting contraction/relaxation measurements. Phenylephrine-induced contraction was allowed to reach a stable plateau. Vasorelaxation was assessed by cumulative addition of acetylcholine (1×10^{-10} M to 1×10^{-5} M).

Statistical Analysis. Data were plotted using GraphPad Prism and RStudio software. Appropriate statistical tests were performed as described in the figure legends. Statistical significance levels are indicated as $*P < 0.05$, $**P < 0.01$, $***P < 0.001$, $****P < 0.0001$; ns, not significant.

Data Availability. Single-cell RNA sequencing data have been deposited in the Gene Expression Omnibus (GEO) database (https://www.ncbi.nlm.nih.gov/geo/) under accession no. GSE142637. All other data from the study are available from R.R.G. and M.J.K. upon request.

ACKNOWLEDGMENTS. We thank the Office of Science and Technology, National Institute of Arthritis and Musculoskeletal and Skin Diseases (NIAMS)/NIH for technical support. This work was supported by the NIH/NIAMS Intramural Research Program (ZIAAR041199) and NIH/National Institute of Diabetes and Digestive and Kidney Diseases IRP (ZO1 DK043308).

1. G. C. Tsokos, Systemic lupus erythematosus. *N. Engl. J. Med.* **365**, 2110–2121 (2011).
2. L. Bennett *et al.*, Interferon and granulopoiesis signatures in systemic lupus erythematosus blood. *J. Exp. Med.* **197**, 711–723 (2003).
3. M. K. Crow, Type I interferon in the pathogenesis of lupus. *J. Immunol.* **192**, 5459–5468 (2014).
4. M. Petri *et al.*, Sifalimumab, a human anti-interferon-α monoclonal antibody, in systemic lupus erythematosus: a phase I randomized, controlled, dose-escalation study. *Arthritis Rheum.* **65**, 1011–1021 (2013).
5. K. C. Kalunian *et al.*, A phase II study of the efficacy and safety of rontalizumab (rhuMAb interferon-α) in patients with systemic lupus erythematosus (ROSE). *Ann. Rheum. Dis.* **75**, 196–202 (2016).
6. M. Khamashta *et al.*; CD1067 study investigators, Sifalimumab, an anti-interferon-α monoclonal antibody, in moderate to severe systemic lupus erythematosus: A randomised, double-blind, placebo-controlled study. *Ann. Rheum. Dis.* **75**, 1909–1916 (2016).
7. R. Furie *et al.*; CD1013 Study Investigators, Anifrolumab, an anti-interferon-α receptor monoclonal antibody, in moderate-to-severe systemic lupus erythematosus. *Arthritis Rheumatol.* **69**, 376–386 (2017).
8. H. M. Lazear, T. J. Nice, M. S. Diamond, Interferon-λ: Immune functions at barrier surfaces and beyond. *Immunity* **43**, 15–28 (2015).
9. S. V. Kotenko, J. E. Durbin, Contribution of type III interferons to antiviral immunity: Location, location, location. *J. Biol. Chem.* **292**, 7295–7303 (2017).
10. H. M. Lazear, J. W. Schoggins, M. S. Diamond, Shared and distinct functions of type I and type III interferons. *Immunity* **50**, 907–923 (2019).
11. S. V. Kotenko *et al.*, IFN-lambdas mediate antiviral protection through a distinct class II cytokine receptor complex. *Nat. Immunol.* **4**, 69–77 (2003).

12. P. Sheppard *et al*., IL-28, IL-29 and their class II cytokine receptor IL-28R. *Nat. Immunol.* **4**, 63–68 (2003).
13. C. Sommereyns, S. Paul, P. Staeheli, T. Michiels, IFN-lambda (IFN-lambda) is expressed in a tissue-dependent fashion and primarily acts on epithelial cells in vivo. *PLoS Pathog.* **4**, e1000017 (2008).
14. A. Broggi, Y. Tan, F. Granucci, I. Zanoni, IFN-λ suppresses intestinal inflammation by non-translational regulation of neutrophil function. *Nat. Immunol.* **18**, 1084–1093 (2017).
15. E. A. Hemann *et al*., Interferon-λ modulates dendritic cells to facilitate T cell immunity during infection with influenza A virus. *Nat. Immunol.* **20**, 1035–1045 (2019).
16. K. Blazek *et al*., IFN-λ resolves inflammation via suppression of neutrophil infiltration and IL-1β production. *J. Exp. Med.* **212**, 845–853 (2015).
17. L. Ye, D. Schnepf, P. Staeheli, Interferon-λ orchestrates innate and adaptive mucosal immune responses. *Nat. Rev. Immunol.* **19**, 614–625 (2019).
18. L. M. Amezcua-Guerra *et al*., Limited effectiveness for the therapeutic blockade of interferon α in systemic lupus erythematosus: A possible role for type III interferons. *Rheumatology (Oxford)* **54**, 203–205 (2015).
19. Q. Wu, Q. Yang, E. Lourenco, H. Sun, Y. Zhang, Interferon-lambda1 induces peripheral blood mononuclear cell-derived chemokines secretion in patients with systemic lupus erythematosus: Its correlation with disease activity. *Arthritis Res. Ther.* **13**, R88 (2011).
20. S. C. Lin, C. C. Kuo, J. T. Tsao, L. J. Lin, Profiling the expression of interleukin (IL)-28 and IL-28 receptor α in systemic lupus erythematosus patients. *Eur. J. Clin. Invest.* **42**, 61–69 (2012).
21. J. Y. Chen *et al*., Interferon-λ3/4 genetic variants and interferon-λ3 serum levels are biomarkers of lupus nephritis and disease activity in Taiwanese. *Arthritis Res. Ther.* **20**, 193 (2018).
22. S. Zahn *et al*., Evidence for a pathophysiological role of keratinocyte-derived type III interferon (IFNλ) in cutaneous lupus erythematosus. *J. Invest. Dermatol.* **131**, 133–140 (2011).
23. A. Zickert *et al*., Interferon (IFN)-λ is a potential mediator in lupus nephritis. *Lupus Sci. Med.* **3**, e000170 (2016).
24. A. Chrysanthopoulou *et al*., Interferon lambda1/IL-29 and inorganic polyphosphate are novel regulators of neutrophil-driven thromboinflammation. *J. Pathol.* **243**, 111–122 (2017).
25. S. Subramanian *et al*., A Tlr7 translocation accelerates systemic autoimmunity in murine lupus. *Proc. Natl. Acad. Sci. U.S.A.* **103**, 9970–9975 (2006).
26. P. Y. Lee *et al*., TLR7-dependent and FcgammaR-independent production of type I interferon in experimental mouse lupus. *J. Exp. Med.* **205**, 2995–3006 (2008).
27. N. Shen *et al*., Sex-specific association of X-linked Toll-like receptor 7 (TLR7) with male systemic lupus erythematosus. *Proc. Natl. Acad. Sci. U.S.A.* **107**, 15838–15843 (2010).
28. K. Sakata *et al*., Up-regulation of TLR7-mediated IFN-α production by plasmacytoid dendritic cells in patients with systemic lupus erythematosus. *Front. Immunol.* **9**, 1957 (2018).
29. M. Souyris *et al*., *TLR7* escapes X chromosome inactivation in immune cells. *Sci. Immunol.* **3**, eaap8855 (2018).
30. M. Yokogawa *et al*., Epicutaneous application of toll-like receptor 7 agonists leads to systemic autoimmunity in wild-type mice: A new model of systemic lupus erythematosus. *Arthritis Rheumatol.* **66**, 694–706 (2014).
31. Y. Liu *et al*., Peptidylarginine deiminases 2 and 4 modulate innate and adaptive immune responses in TLR-7-dependent lupus. *JCI Insight* **3**, 124729 (2018).
32. W. Li, A. A. Titov, L. Morel, An update on lupus animal models. *Curr. Opin. Rheumatol.* **29**, 434–441 (2017).
33. X. Huang, S. Dorta-Estremera, Y. Yao, N. Shen, W. Cao, Predominant role of plasmacytoid dendritic cells in stimulating systemic autoimmunity. *Front. Immunol.* **6**, 526 (2015).
34. R. R. Goel *et al*., Interferon lambda promotes immune dysregulation and tissue inflammation in TLR7-induced lupus [scRNA-seq]. Gene Expression Omnibus. https://www.ncbi.nlm.nih.gov/geo/query/acc.cgi?acc=GSE142637. Deposited 26 December 2019.
35. A. Kelly *et al*., Immune cell profiling of IFN-λ response shows pDCs express highest level of IFN-λR1 and are directly responsive via the JAK-STAT pathway. *J. Interferon Cytokine Res.* **36**, 671–680 (2016).
36. E. Der *et al*.; Accelerating Medicines Partnership Rheumatoid Arthritis and Systemic Lupus Erythematosus (AMP RA/SLE) Consortium, Tubular cell and keratinocyte single-cell transcriptomics applied to lupus nephritis reveal type I IFN and fibrosis relevant pathways. *Nat. Immunol.* **20**, 915–927 (2019).
37. L. C. Tsoi *et al*., Hypersensitive IFN responses in lupus keratinocytes reveal key mechanistic determinants in cutaneous lupus. *J. Immunol.* **202**, 2121–2130 (2019).
38. K. Witte *et al*., Despite IFN-lambda receptor expression, blood immune cells, but not keratinocytes or melanocytes, have an impaired response to type III interferons: Implications for therapeutic applications of these cytokines. *Genes Immun.* **10**, 702–714 (2009).
39. S. G. Thacker *et al*., Type I interferons modulate vascular function, repair, thrombosis, and plaque progression in murine models of lupus and atherosclerosis. *Arthritis Rheum.* **64**, 2975–2985 (2012).
40. I. Zanoni, F. Granucci, A. Broggi, Interferon (IFN)-λ takes the helm: Immunomodulatory roles of type III IFNs. *Front. Immunol.* **8**, 1661 (2017).
41. V. Espinosa *et al*., Type III interferon is a critical regulator of innate antifungal immunity. *Sci. Immunol.* **2**, eaan5357 (2017).
42. R. A. de Groen, Z. M. Groothuismink, B. S. Liu, A. Boonstra, IFN-λ is able to augment TLR-mediated activation and subsequent function of primary human B cells. *J. Leukoc. Biol.* **98**, 623–630 (2015).
43. J. Wenzel *et al*., Enhanced type I interferon signalling promotes Th1-biased inflammation in cutaneous lupus erythematosus. *J. Pathol.* **205**, 435–442 (2005).
44. P. Enghard *et al*., CXCR3+CD4+ T cells are enriched in inflamed kidneys and urine and provide a new biomarker for acute nephritis flares in systemic lupus erythematosus patients. *Arthritis Rheum.* **60**, 199–206 (2009).
45. O. M. Steinmetz *et al*., CXCR3 mediates renal Th1 and Th17 immune response in murine lupus nephritis. *J. Immunol.* **183**, 4693–4704 (2009).
46. N. Ank *et al*., Lambda interferon (IFN-lambda), a type III IFN, is induced by viruses and IFNs and displays potent antiviral activity against select virus infections in vivo. *J. Virol.* **80**, 4501–4509 (2006).
47. M. C. Lebre *et al*., Human keratinocytes express functional toll-like receptor 3, 4, 5, and 9. *J. Invest. Dermatol.* **127**, 331–341 (2007).
48. A. Forero *et al*., Differential activation of the transcription factor IRF1 underlies the distinct immune responses elicited by type I and type III interferons. *Immunity* **51**, 451–464.e6 (2019).
49. Z. Zhou *et al*., Type III interferon (IFN) induces a type I IFN-like response in a restricted subset of cells through signaling pathways involving both the Jak-STAT pathway and the mitogen-activated protein kinases. *J. Virol.* **81**, 7749–7758 (2007).
50. Y. Furumoto *et al*., Tofacitinib ameliorates murine lupus and its associated vascular dysfunction. *Arthritis Rheumatol.* **69**, 148–160 (2017).
51. D. J. Wallace *et al*., Baricitinib for systemic lupus erythematosus: A double-blind, randomised, placebo-controlled, phase 2 trial. *Lancet* **392**, 222–231 (2018).
52. J. D. Lin *et al*., Distinct roles of type I and type III interferons in intestinal immunity to homologous and heterologous rotavirus infections. *PLoS Pathog.* **12**, e1005600 (2016).
53. T. Stuart *et al*., Comprehensive integration of single-cell data. *Cell* **177**, 1888–1902.e21 (2019).
54. D. Aran *et al*., Reference-based analysis of lung single-cell sequencing reveals a transitional profibrotic macrophage. *Nat. Immunol.* **20**, 163–172 (2019).
55. U. Lichti, J. Anders, S. H. Yuspa, Isolation and short-term culture of primary keratinocytes, hair follicle populations and dermal cells from newborn mice and keratinocytes from adult mice for in vitro analysis and for grafting to immunodeficient mice. *Nat. Protoc.* **3**, 799–810 (2008).
56. A. Uchiyama *et al*., SOX2 epidermal overexpression promotes cutaneous wound healing via activation of EGFR/MEK/ERK signaling mediated by EGFR ligands. *J. Invest. Dermatol.* **139**, 1809–1820.e8 (2019).